

RESEARCH ARTICLE

CRPS chart: Simultaneously monitoring location and scale under data-rich environment

Liangxing Shi¹ | Ling Gong¹ | Dennis K.J. Lin²

¹Department of Industrial Engineering,
Tianjin University, Tianjin, China

²Department of Statistics, The
Pennsylvania State University, PA, USA

Correspondence

Liangxing Shi, Department of Industrial
Engineering, Tianjin University, 300072,
Tianjin, China.
Email: shi@tju.edu.cn

Funding information

National Natural Science Foundation of
China, Grant/Award Number: 71532008

Abstract

The detection performance of a conventional control chart is usually degraded by a large sample size as in Wang and Tsung. This paper proposes a new control chart under data-rich environment. The proposed chart is based on the continuous ranked probability score and aims to simultaneously monitor the location and the scale parameters of any continuous process. We simulate different monitoring schemes with various shift patterns to examine the chart performance. Both in-control and out-of-control performances are studied through simulation studies in terms of the mean, the standard deviation, the median, and some percentiles of the average run length distribution. Simulation results show that the proposed chart keeps a high sensitivity to shifts in location and/or scale without any distributional assumptions, and the outperformance improves, as the sample size becomes larger. Examples are given for illustration.

KEYWORDS

average run length, CRPS, data-rich environment, large sample size, location and scale

1 | INTRODUCTION

Statistical process control has received extensive attention for a long period and keeps evolving to meet the needs of various industries. With the development of modern measurement and inspection technology, such as the machine vision systems and other high-frequency in-process sensing technology, large amounts of process data are often available within short time intervals. A typical example, provided by Wang and Tsung,¹ is that “since the in-line Optical Coordinate Measurement Machine needs to measure 100-150 points on each major assembly with a 100% sample rate, a tremendous amount of measurement data would be generated every 10-30 seconds.” Another example given there is the cellular phone display, which is tested by a machine vision system during its production process. Since every image contains nearly 1000 pixels, 1 display is a sample with 1000 independent observations. For the incoming big data era, how to make a good use

of those large amounts of data becomes a real challenge for modern statistical process control techniques.

Compared with the existing control charts that only monitor a single process parameter (location or scale), control charts that simultaneously monitor both of the location and scale are considered to be more reasonable and effective. Simultaneous shifts in both the location and scale are likely to happen because a shift in one of the parameters usually affects the other. Taking the normal distribution for instance, control limits of the mean chart may no longer be effective because of the influence of shifts in the variance, thus dramatically impacting the chart performance. Gan et al² pointed out that it is more reasonable to combine the mean and variance information on 1 scheme and study their behavior simultaneously.

Here, we focus on developing a new control chart for simultaneously monitoring the location and scale under data-rich environment. The existing methods for handling large sample size are to calculate sufficient statistics (such

as the mean or variance). However, Wang and Tsung¹ noted that this approach may sometimes ignore some serious defects that are due to partial out-of-control data in a sample, as the out-of-control data would be averaged out and buried in the large sample. To address this concern, we propose to characterize each sample by the continuous ranked probability score (CRPS) statistic, which has low sensitivity to the increasing sample size and thus is appropriate for data-rich monitoring situations. Moreover, a CRPS-based control chart, which simultaneously monitors shifts in the location and/or the scale without distributional assumptions, is proposed.

The rest of the article is organized as follows. Section 2 reviews the current available literature on simultaneously monitoring the location and scale. Preliminaries of the CRPS method are given in Section 3. The proposed CRPS chart is introduced in Section 4, including the determinations of control limits and the charting procedure. Section 5 illustrates examples with small and large sample sizes to show how the proposed CRPS chart is implemented in practice. Section 6 shows the in-control and out-of-control performances of the CRPS chart in terms of different shift patterns and different sample sizes. Performance comparisons with both the parametric likelihood ratio-based EWMA chart (denoted by ELR chart) and nonparametric Shewhart-Laplace (SL) and Shewhart-Cuconci (SC) charts are also provided there. Section 7 gives some conclusions.

2 | LITERATURE REVIEW

Basically, there are 2 main approaches to simultaneously monitoring the location and scale. The first approach uses 2 independent control charts to monitor the location and scale, such as the conventional \bar{X} & R chart. The second approach is to construct a single control chart by using an integrated plotting statistic or 2 independent plotting statistics. A single chart is much simpler to use and has better performance. As noted by McCracken and Chakraborti,³ the overall false alarm rate of the 2-chart control schemes could be twice as high as the 1-chart control schemes. See, for example, Chowdhury et al,⁴ Chen and Cheng,^{5,6} Costa and Rahim,⁷ Yeh et al,⁸ Zhang et al,⁹ and reviews on the subject by Cheng and Thaga,¹⁰ and McCracken and Chakraborti.³

A vast majority of the existing 1-chart joint monitoring schemes assume a normal distribution of the underlying data. However, data in practice are more likely not normally distributed. It is desirable to develop monitoring schemes that do not rely on normality. Some examples are as follows. Zou and Tsung¹¹ proposed a distribution-free EWMA control chart that integrates Zhang's¹²

goodness-of-fit test and EWMA process monitoring. They show that the proposed scheme is efficient in detecting shifts in location or scale, when the underlying process distribution is unknown. Mukerjee and Chakraborti¹³ developed a distribution-free SL chart with a charting statistic based on the Lepage¹⁴ statistic, which combines the Wilcoxon rank sum test for location and the Ansari-Bradley test for scale. Although the SL chart is able to monitor the location and the scale parameters for any continuous process, 1 limitation there is that it is not capable for detecting changes in the shape. Chowdhury et al¹⁵ extended the work to present a similar distribution-free control chart to monitor the location and scale simultaneously. The proposed SC chart is based on the Cucconi¹⁶ statistic, and they show by simulations that their chart performs just as well or better than the SL chart. However, the problem of detecting shifts in the shape still remains primitive.

As previously mentioned, the amount of data is usually very large in the modern manufacturing process. However, little research really looks into how to make full use of those high-volume data to simultaneously monitor the location and scale under data-rich environment. In this paper, we develop a distribution-free control chart to simultaneously monitor the location and the scale for the data-rich problem. For simplicity, we assume that in-control samples can be obtained from a phase 1 study.

3 | PRELIMINARIES FOR USING CRPS

The CRPS (see Brown¹⁷) is a kind of scoring and verification tool. It was originally developed for probabilistic forecast systems to evaluate how accurately the forecast system can describe the occurrence and nonoccurrence of a certain event, mainly by measuring the difference between the predicted and occurred cumulative distribution functions (CDFs; see Hersbach,¹⁸ Thorarinsdottir and Gneiting,¹⁹ and Pinson et al²⁰). Since the CRPS method effectively calculates the distance from a distribution to a certain point, it is now commonly used for many functions beyond forecasting. For example, Shi et al²¹ proposed a CRPS-based approach to analyze the process capability and showed that their method is applicable to both normal and nonnormal cases. Basically, the CRPS statistic is defined as

$$CRPS = S(F, y) = \int_{-\infty}^{+\infty} (F(t) - H(t-y))^2 dt \quad (1)$$

Here y is the desired value and t is the observed value; $S(F, y)$ is the CRPS value obtained by computing the integral of the square difference between F and H ;

F and H are 2 CDFs, among which H is the Heaviside function, that is, $H(x-y) = \begin{cases} 0 & t < y \\ 1 & t \geq y \end{cases}$.

Shi et al²¹ demonstrated that CRPS can also be expressed as

$$\begin{aligned} S(F, y) &= \int_{-\infty}^y (F(t))^2 dt + \int_y^{+\infty} (F(t)-1)^2 dt \\ &= S_l(F, y) + S_u(F, y) \end{aligned} \quad (2)$$

Here $S_l(F, y)$ is the CRPS value below y , and $S_u(F, y)$ is the CRPS value beyond y . Since the CRPS value measures the dispersion of any continuous process, a smaller CRPS value obviously indicates a smaller gap between the desired and observed value, indicating a more capable process, while large values indicate processes that are out of control. A minimal CRPS value of zero is only obtained when $F = H$, representing the ideal situation where the observed process successfully produced an ideal part.

Friedman²² and Nau²³ pointed out the relationship between CRPS and distances $S(F, y) \geq S(G, y) \Leftrightarrow d(f, y) \geq d(g, y)$. Here d represents an arbitrary kind of distance metric that satisfies 3 conditions: nonnegative, symmetric, and the triangle inequality, for any 2 probability density functions f and g , F and G being their corresponding CDFs. With this encouraging discovery, we are able to use the CRPS to compare the performance of different distributions. To illustrate the effectiveness without any constraints on data distribution, various simulations have been conducted, including normal distribution and nonnormal distributions.

3.1 | Normal distribution

For each scenario below, 1000 random numbers are generated for different types of shifts on the CRPS value. Each simulation is studied with 3 replicates, and results of all obtained CRPS values are displayed in Table 1. Their corresponding Probability Density Function (PDF) and CDF for an intuitive interpretation of the corresponding CRPS

values were then plotted, as shown in Figure 1, where the CRPS values are presented as the shaded area between CDF and y . Four scenarios are reported here:

- Process in-control. Assume that the controlled process follows the standard normal distribution, and 1000 random numbers that follow this distribution are generated. It is shown that the variation among CRPS values is very small when the desired value y is considered to be the process mean 0.
- A shift in the location. Assume that the process is currently out of control due to a shift in the location which increases the mean from 0 to 1 and preserves the variance simultaneously. It is easy to see that this shift has a great impact on the corresponding CRPS value, which is more than the double of that in the first situation.
- A shift in the scale. Similarly, assume there is a shift in the scale, which increases the process variance from 1 to 2, while the process mean is preserved. Here, the CRPS value also shows a great difference with the 2 situations above.
- Shifts in both the location and scale. When there is a shift in both the location and scale, take an increase in the mean from 0 to 1 and meanwhile an increase in the variance from 1 to 2. Table 1 shows that the CRPS value has increased even more compared with the above 3 situations, which can be simply interpreted as a combined effect caused by the location and scale shifts.

3.2 | Nonnormal distribution

When the normality assumption is invalid, for example, a skewed or a heavier tailed distribution, the above 4 situations are also studied to show that similar influence also appears for nonnormal cases. For simplicity, we only take

TABLE 1 CRPS values for different shifts in a normal process

Times	(a) $\theta = 0, \sigma = 1$			(b) $\theta = 1, \sigma = 1$		
	1	2	3	1	2	3
$S_l(F, y)$	0.111	0.098	0.117	0.006	0.006	0.006
$S_u(F, y)$	0.109	0.118	0.098	0.583	0.589	0.581
$S(F, y)$	0.220	0.216	0.215	0.589	0.595	0.587
Times	(c) $\theta = 0, \sigma = 2$			(d) $\theta = 1, \sigma = 2$		
	1	2	3	1	2	3
$S_l(F, y)$	0.230	0.212	0.204	0.059	0.063	0.064
$S_u(F, y)$	0.200	0.216	0.232	0.578	0.566	0.552
$S(F, y)$	0.430	0.428	0.436	0.636	0.629	0.616

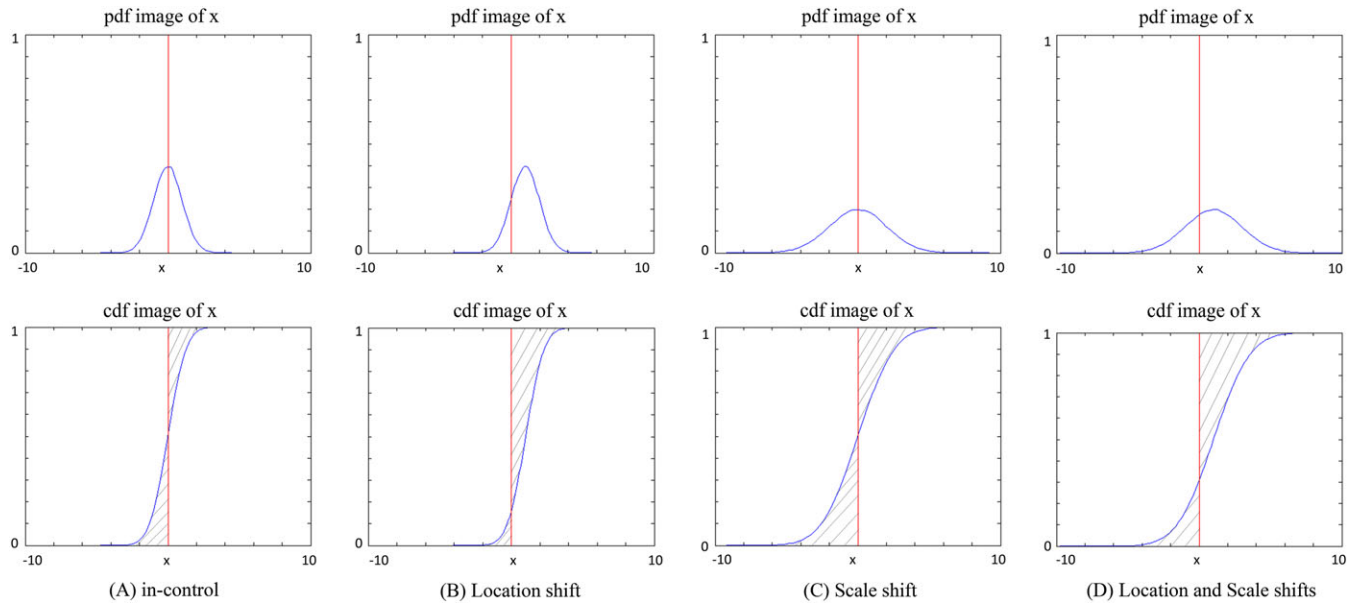


FIGURE 1 Schematic diagrams of CRPS for different types of shifts in a normal process [Colour figure can be viewed at wileyonlinelibrary.com]

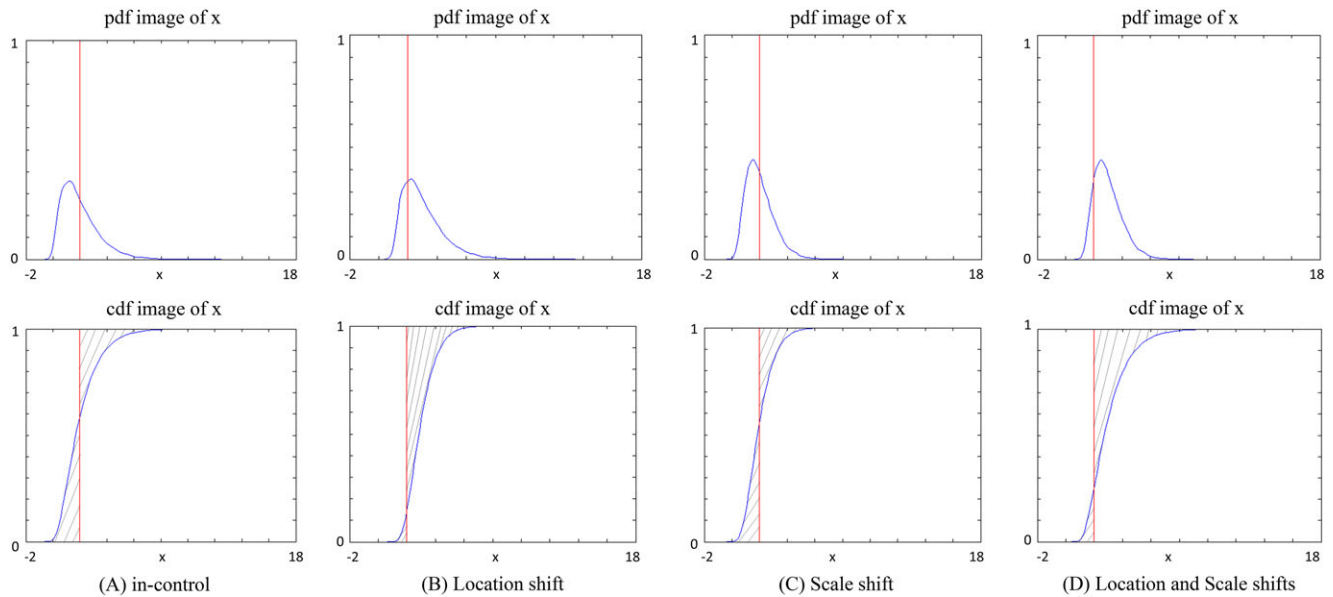


FIGURE 2 Schematic diagrams of CRPS for different types of shifts in a gamma process [Colour figure can be viewed at wileyonlinelibrary.com]

the heavy-tailed gamma distribution as example. Simulations are done using the same method as the normal case. The simulation results are displayed in Figure 2A to D. For each situation, results of all obtained CRPS values are shown in Table 2, from which we can also see that the variation of CRPS values is small within the same situation. However, when shifts occur, whether location shift or scale shift or both, there is a great effect on the CRPS value.

- a. Process in-control. We simulate a controlled process that follows a gamma distribution with the shape parameter $\alpha = 2$ and the scale parameter $\beta = 1$. Then 1000 random numbers are generated. The desired value y for CRPS is the in-control process mean, which equals to 2.
- b. A shift in the location. Assume there is a shift in the location, which moves all those random numbers generated in the first situation 1 unit to the right.

TABLE 2 CRPS values for different shifts in a gamma process

Times	(a) $\alpha = 2, \beta = 1$			(b) $\alpha = 2, \beta = 1$ move (a) 1 unit to the right		
	1	2	3	1	2	3
$S_i(F, y)$	0.2087	0.2042	0.2206	0.0150	0.0142	0.0126
$S_u(F, y)$	0.1001	0.1018	0.0959	0.4054	0.4147	0.4211
$S(F, y)$	0.3088	0.3060	0.3164	0.4204	0.4289	0.4337
Times	(c) $\alpha = 4, \beta = 1/2$			(d) $\alpha = 4, \beta = 1/2$ move (c) 1 unit to the right		
	1	2	3	1	2	3
$S_i(F, y)$	0.1175	0.1324	0.1199	0.0021	0.0024	0.0035
$S_u(F, y)$	0.0956	0.0789	0.0934	0.5064	0.5234	0.4781
$S(F, y)$	0.2131	0.2114	0.2133	0.5085	0.5258	0.4816

For comparison, the corresponding CRPS values are calculated with the same desired value $y = 2$.

- c. A shift in the scale. In this scenario, to ensure that there are no shifts in location but only in scale, we generate 1000 random numbers from a gamma distribution with parameters $\alpha = 4$ and $\beta = 1/2$.
- d. Shifts in both the location and scale. To shift both location and scale, again we use gamma distribution with parameters $\alpha = 4$ and $\beta = 1/2$, but move those random numbers generated in the third situation 1 unit to the right.

Through the analysis of the normal and nonnormal cases, it is shown that the CRPS value can effectively identify changes in both the location and scale regardless the underlying distribution. Since CRPS considers all available points by calculating its CDF, it gives a complete indication of process variation, which can be beneficial for quality control. In addition, the CRPS approach is expected to become more sensitive to shifts when there are more data in the sample.

4 | CONSTRUCTION OF THE CRPS CHART

4.1 | Determinations of control limits

When determining the control limits of the chart, the key problem is to find the reasonable range of CRPS values from an in-control process. Thus, an out-of-control process can be indicated whenever the CRPS value is out of the given range. In this paper, we determine the control limits by the following steps: First, collect k reference samples $X = (x_1, \dots, x_i, \dots, x_k)$ from historical data which all stem from an in-control process. Each sample includes multiple independent observations, and the sample size is denoted by m . That is, $x_i = (d_1, \dots,$

$d_j, \dots, d_m)$. Second, calculate the corresponding CRPS value for each sample in X . Third, analyze the CRPS distribution with the obtained k CRPS values, so control limits can be finally determined.

To gain a general understanding of the CRPS distribution, we conducted the following simulation experiments with 3 representative distributions: normal, exponential, and bimodal distributions are studied respectively. For each scenario, 10 000 samples are generated from the corresponding population distributions. The sample size m is respectively set at 10, 25, 50, 75, and 100 to study the impact of sample size on the CRPS distribution. Figures 3–5 show the PDF of each considered distribution, as well as the CRPS distribution obtained by the corresponding samples with different sizes. It is shown that the CRPS distribution is similar to the normal distribution in all scenarios, especially when m is larger than about 100. Clearly, regardless the underlying distribution, the CRPS distribution has a similar pattern with the normal distribution, and this characterization is becoming more stable with an increasing sample size m .

We then use the parameter estimation method to approximate the exact distribution function of CRPS. Since our empirical (simulation) observations indicate that Gamma distribution could be an ideal approximation for the CRPS distribution, we use the maximum likelihood estimation method to estimate the shape parameter α and scale parameter β of the gamma distribution. Therefore, control limits can be determined by choosing an acceptable false alarm rate. The acceptable in-control average run length (denoted by ARL_0) can be found for any lower control limit (LCL) and upper control limit (UCL) by Equations 3 and 4. It is worth mentioning that the right side of the equations is the CDF of a gamma distribution while the acceptable ARL_0 appears on the left. Finally, by setting the ARL_0 equals to some desired value ARL_0^* , control limits can be determined by solving

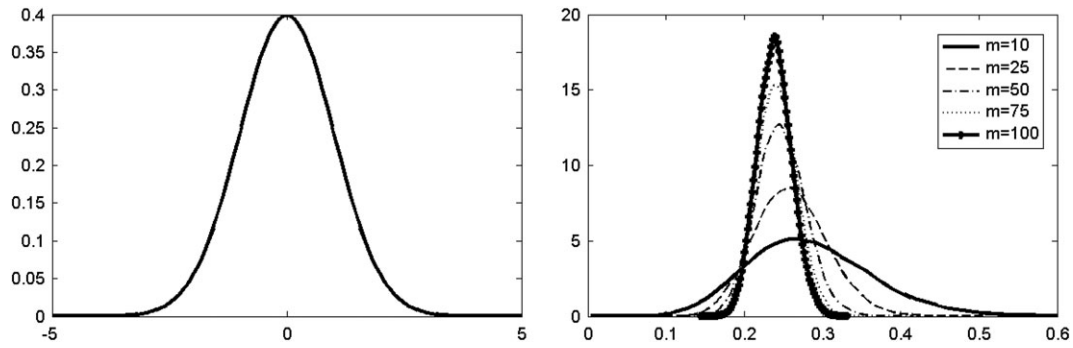


FIGURE 3 Standard normal distribution population (left) and corresponding CRPS distributions with different sample size m (right)

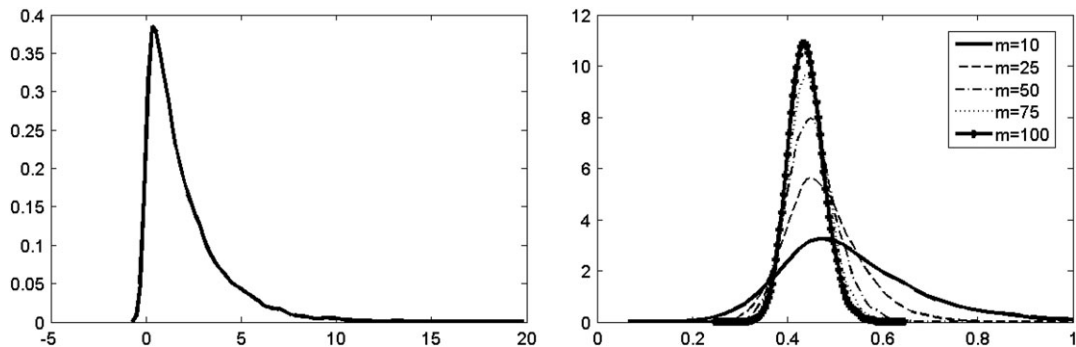


FIGURE 4 Exponential distribution population (left) and corresponding CRPS distributions with different sample size m (right)

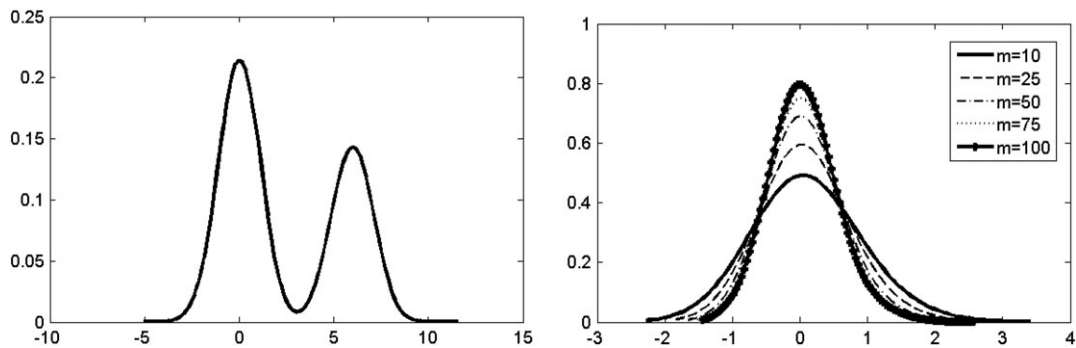


FIGURE 5 Bimodal distribution population (left) and corresponding CRPS distributions with different sample size m (right)

$$\frac{1}{2ARL_0^*} = \int_{LCL}^{\infty} \frac{x^{(\hat{\alpha}-1)} \left(1/\hat{\beta}\right)^{\hat{\alpha}} e^{-x/\hat{\beta}}}{\Gamma(\hat{\alpha})} dt \quad (3)$$

$$1 - \frac{1}{2ARL_0^*} = \int_{-\infty}^{UCL} \frac{x^{(\hat{\alpha}-1)} \left(1/\hat{\beta}\right)^{\hat{\alpha}} e^{-x/\hat{\beta}}}{\Gamma(\hat{\alpha})} dt \quad (4)$$

Here $\hat{\alpha}$ and $\hat{\beta}$ are the maximum likelihood estimation of α and β . To get the solutions, simulations are called for. Since the CRPS method is distribution-free, data are

generated from the standard normal distribution. For parameters selection, assume that 100 reference samples are collected in the historical data (the more, the better), and the sample size m is set at 50, 100, 300, and 500. In addition, ARL_0^* is selected to be 250, 370, and 500. Each simulation is done with 1000 replications. Results are shown in Table 3.

Table 3 shows that as m increases, the distance between LCL and UCL decreases under the same ARL_0^* . Figure 6 gives the profiles of various m and its corresponding limits when $ARL_0^* = 370$, which indicates that although the LCL-UCL range continues to narrow as m approaches 200, the increases are no longer as dramatic.

When m increases beyond about 200, there is very little change. This means that the CRPS chart becomes stable with larger sample cases. This characteristic is especially meaningful for data-rich environments, since it is increasingly common in practice for large amounts of process data to be generated over short time intervals.

4.2 | Procedure for the CRPS chart

The proposed CRPS chart can be constructed as follows.

1. Collect reference samples $X = (x_1, x_2, \dots, x_k)$ from the in-control process, and use $x_i = (d_1, d_2, \dots, d_m)$ represents the i th subgroup.
2. Calculate the CRPS values for each sample in X , determine the lower limit LCL, and the upper limit UCL using Equations 3 and 4 in (4.1); thus, the CRPS chart is constructed.
3. Collect test samples $Y = (y_1, y_2, \dots, y_m)$ at regular time intervals from the current unknown process. Assume that the sample size is m . Let $y_j = (e_1, e_2, \dots, e_m)$ represent the j th test sample.
4. Calculate the CRPS values for each test sample in Y and then display them on the constructed CRPS chart.
5. If the CRPS value of the j th test sample exceeds LCL or UCL, the process is declared out-of-control at the j th sample. If not, the process is considered to be in-control and we continue to test the next sample.

5 | ILLUSTRATIVE EXAMPLE

Three case studies are given here to show how the proposed CRPS chart can be implemented in practice. Section 5.1 studies the piston ring data with small sample ($m = 5$) to facilitate the comparison with the SL and SC charts (Mukerjee and Chakraborti¹³ and Chowdhury et al¹⁵). Section 5.2 studies the indoor noise detection data with a sample size $m = 300$, which illustrates that the CRPS chart is also effective when the sample size is greatly increased. Section 5.3 studies the machine vision

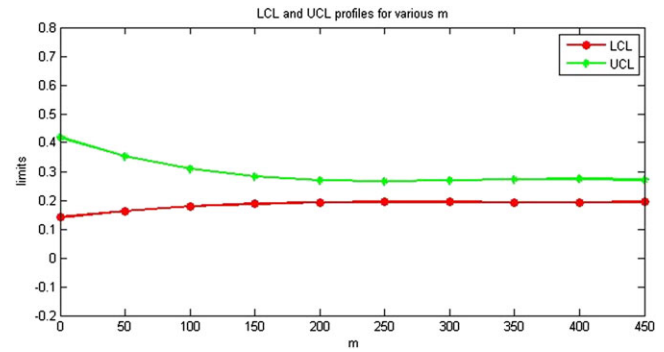


FIGURE 6 LCL and UCL profiles for various values m when $ARL_0^* = 370$ [Colour figure can be viewed at wileyonlinelibrary.com]

system, using a real industrial nonwoven textile image that contains 62 500 pixels ($m = 62\,500$) to show the CRPS chart for the data-rich environment.

5.1 | Example of piston ring data

The well-known piston ring data discussed in Montgomery²⁴ are used to make a comparison among the performance of CRPS chart with that of the SL and SC charts. With the given 25 reference samples of inside diameter measurements of forged automobile engine piston rings, there are 5 piston rings in each sample. Another 15 subgroups with the same sample size are also provided as the test samples. Thus, $k = 25$ and $m = 5$. What we need to do is to judge whether the current process is in-control or out-of-control and detect shifts in the process as early as possible.

Following our proposed charting procedure, first the corresponding CRPS value for each reference sample should be calculated with a desired value y equal to the mean value 74.000. Then, the maximum likelihood estimation method is adapted to gain the control limits of the chart, and the results are $LCL = 0.00063$, $UCL = 0.0092$ for a target ARL_0^* of 500. We next calculate the corresponding CRPS value for each test sample. Finally, by plotting the obtained CRPS values on the constructed CRPS chart (see Figure 7), we are able to make a judgment that the 12th sample is out-of-control.

TABLE 3 LCL and UCL of the CRPS chart for selective m

m	$ARL_0^* = 250$		$ARL_0^* = 370$		$ARL_0^* = 500$	
	LCL	UCL	LCL	UCL	LCL	UCL
50	0.16605	0.34811	0.16313	0.35296	0.16100	0.35658
100	0.18048	0.30623	0.17828	0.30938	0.17667	0.31173
300	0.19509	0.26692	0.19373	0.26861	0.19272	0.26986
500	0.19943	0.25520	0.19835	0.25648	0.19755	0.25744

Clearly, the CRPS value of the first 11 test samples are all within the scope of LCL and UCL, while the 12th test sample is the first sample beyond the control limits. Note that this is consistent with the SL and SC charts.

5.2 | Example of indoor environmental noise

The mobile app Noise Detector installed in smartphones is used to monitor its indoor environmental noises. We assume that the changes of noises are under control when the air conditioning is turned off, and it becomes out-of-control when the air conditioning is turned on. Apart from the air conditioning, all other factors that may influence the indoor noise value are controlled at the same level. We next illustrate the proposed CRPS chart under data-rich environment with large sample size by conducting an experiment of indoor noise detection.

The air conditioning is first turned off, and the detection frequency of the mobile app Noise Detector is set at 1 Hz. The decibel value of indoor noise is measured per second by this app. We made continuous measurement for 5 minutes each time; thus, a total of 300 observations were obtained each time. That is, the reference sample size $m = 300$. The whole experiment was conducted for 10 times with intervals of every hour, so 10 reference samples with sample size $m = 300$ were finally collected. Next, the air conditioning was turned on, and we began to collect test samples using the same app Noise Detector. The sample size was also 300, and we collected 5 test samples in this experiment. Finally, the proposed CRPS chart is

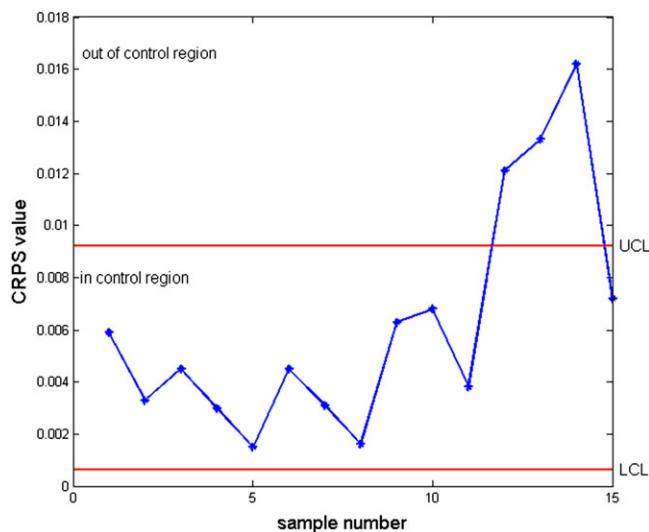


FIGURE 7 CRPS chart for the piston ring data [Colour figure can be viewed at wileyonlinelibrary.com]

used to find whether it is able to identify changes in the indoor noises.

The desired value y for CRPS value is taken as the population mean of all obtained in-control samples. This can be estimated by the sample mean of $\bar{y} = 63.50$. Based on this, we calculate the CRPS values for each reference sample, and the results are 1.7828, 1.5391, 1.4824, 1.5762, 1.437, 1.3291, 1.482, 0.8781, 1.3528, and 1.7684. Then, the LCL and UCL are respectively found to be 0.782 and 2.412 with a target ARL_0^* set at 500. Finally, the CRPS values of each test sample are calculated (with a same y value). Results of first 3 test samples are 2.4735, 3.9282, and 4.9075. Figure 8 displays all the CRPS values on the CRPS chart. The chart immediately indicates an out-of-control signal at the 11th sample. This is indeed the time point when we turned on the air-conditioning.

5.3 | Example of nonwoven textile images

A sample of nonwoven textile images in Megahed et al²⁵ is used to illustrate the problem in a data-rich environment. The nonwoven textile testing process is a specific application of machine vision system in industrial production practice. The traditional manual visual is hard to evaluate the quality of produced nonwoven textiles and to judge whether the process maintains a similar pattern. Therefore, image acquisition devices (working at high speed) capture the product images and send them to a software system to analyze.

Here, we are interested in using the proposed CRPS chart to detect faults in nonwoven textile images. An industrially produced nonwoven image that contains

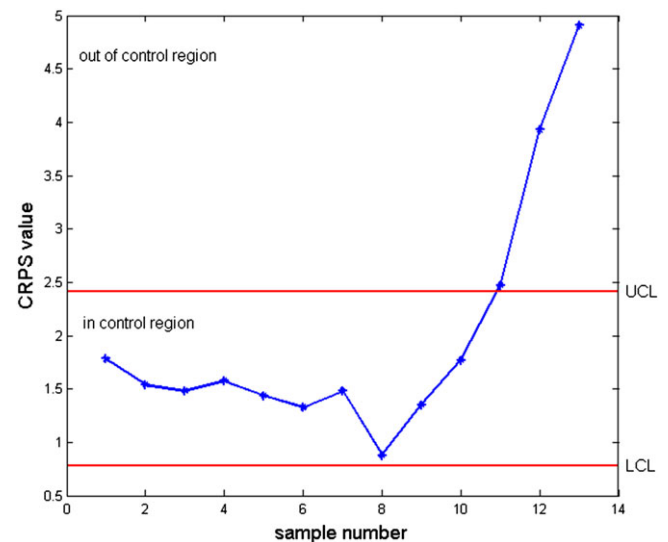


FIGURE 8 CRPS chart for the indoor noise data [Colour figure can be viewed at wileyonlinelibrary.com]

62 500 (250×250) pixels is used, and each pixel is independent of other pixels. A nonwoven textile image is thus a sample with 62 500 independent observations. Under the in-control status, each pixel follows a normal distribution and all produced nonwoven textile images follow a specific pattern. In our simulation study, we first used the real industrial image to generate 1000 similar images by adding Gaussian noise, with mean 0 and the standard deviation 1. We then calculate the CRPS value of 62 500 pixel values for each obtained in-control nonwoven textile image. According to the proposed monitoring scheme, the desired value y for calculating the CRPS value is taken as the population mean of all obtained pixels in the in-control images, and this is estimated by the sample mean of $\bar{y} = 128.03$. Based on this, we are able to obtain 1000 CRPS values. The LCL and UCL of CRPS chart are respectively found to be 38.63 and 39.31 with a target ARL_0^* of 370 (see Section 4.1 for details).

Under the out-of-control status, a shift in location and/or scale may happen in the process at a certain moment. This will lead to defective nonwoven textiles. In the simulation experiment, this situation can be generated by adding a Gaussian noise with a different mean and standard deviation. For simplicity, only a location shift is considered here. To obtain the out-of-control samples, we add a Gaussian noise with its mean equals to 0.2 and the standard deviation remains 1 to the real textile image. First, 10 in-control images and 5 out-of-control images are generated. Then, we calculated its corresponding CRPS values. Results are 38.9592, 38.9987, 38.9270, 39.0904, 38.9304, 38.9735, 38.7356, 38.9201, 38.8985, 38.8084, 40.1016, 39.9594, and 40.0724. Since the control limits were found to be 38.63 and 39.31, all obtained CRPS values can be placed on the CRPS chart, as displayed in Figure 9. The chart immediately indicates an out-of-control signal at the 11th sample. This is the exact time point where a different Gaussian noise is added.

6 | PERFORMANCE ANALYSIS AND COMPARISON

The distribution of average run length is commonly used to evaluate the performance of a control chart. Meanwhile, various summary measures such as the mean, the standard deviation (SD), and several percentiles including the 5th percentile, the 25th percentile, median, the 75th percentile, and the 95th percentile are also studied here to evaluate the chart performance. First we consider the in-control performance in Section 6.1, and then out-of-control performance is analyzed in Section 6.2. Finally, performance comparisons of the CRPS chart among the

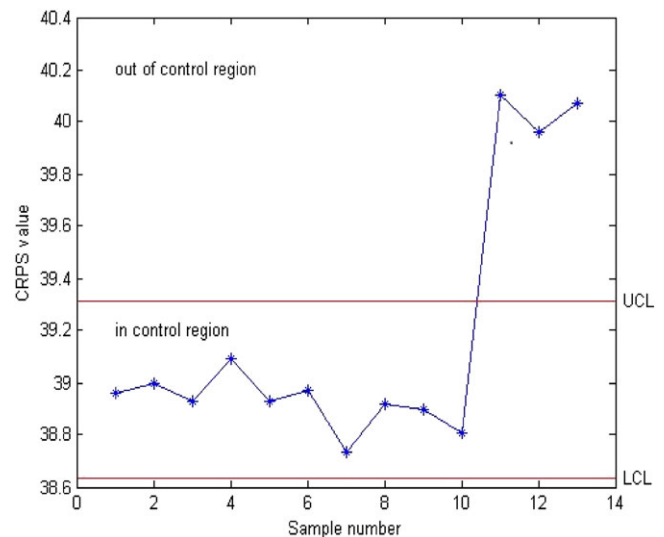


FIGURE 9 CRPS chart for the nonwoven images [Colour figure can be viewed at wileyonlinelibrary.com]

parametric ELR chart and nonparametric SL and SC charts are provided in Section 6.3.

6.1 | In-control performance analysis

For in-control case, we study the in-control average run length ARL_0 distribution by simulation. Both reference and test samples are simulated from the standard normal distribution. Taking $k = 100$ and $ARL_0^* = 370$, for example, we choose different m to be 50, 100, 300, and 500. Control limits for each given m with 1000 replications are obtained in Table 3, with summary measures related to ARL_0 are shown in Table 4. For each m value, the median is much smaller than the mean value, which indicates that ARL_0 is skewed to the right. For example, when $m = 50$, the mean value of ARL_0 is nearly 1.5 times larger than the median. Moreover, as m becomes larger, the mean value of ARL_0 is getting closer to the desired value 370, and it remains about 370 when m is larger than 500. This indicates that the proposed CRPS chart has a better in-control performance for larger sample sizes.

6.2 | Out-of-control performance analysis

To study the out-of-control performance of the CRPS chart, we study how the chart behaves when there are shifts in location, scale, and both the location and scale. We consider the following 2 cases: (1) the thin-tailed symmetric normal distribution $N(\theta, \sigma)$ and (2) the heavy-tailed symmetric Laplace distribution $Laplace(\theta, \sigma)$. In both cases, note that θ reflects the offset quantity of the location parameter, and σ represents the degree of deviation

TABLE 4 In-control performance characteristics of ARL_0 for a normal distribution with $ARL_0^* = 370$

m	LCL	UCL	Simulated Values						
			Mean	SD	5th	25th	Median	75th	95th
50	0.16313	0.35296	326.61	335.21	15.5	93	224.5	445.5	1037.5
100	0.17828	0.30938	341.80	328.81	18.5	100	237	504.5	1022
300	0.19373	0.26861	353.86	339.96	21	101	249.5	493	1037
500	0.19835	0.25648	364.75	366.85	20.5	96	249	497.5	1166.5

for the scale parameter. We simulated different combinations for θ and σ in each case.

In the first case, the out-of-control samples are generated from an $N(\theta, \sigma)$ distribution while in-control samples come from a standard normal distribution. We considered 25 combinations of (θ, σ) values via $\theta = 0, 0.1, 0.2, 0.3, 0.4$ and $\sigma = 1, 1.1, 1.2, 1.3, 1.4$. Taken $k = 100$ and $ARL_0^* = 370$, control limits are available by Table 3. Each simulation is repeated with 1000 replications. Results for $m = 50, 500$ are given in Tables A1 and A2, respectively. Figure 10 shows the profiles of out-of-control average run length (ARL_1) as θ/σ increases for a given number of σ/θ values. Among them, Figure 10A,B gives the profiles of ARL_1 when $m = 50$; and Figure 10C,D shows the results for $m = 500$. In general, the simulation results show that (i) ARL_1 distributions are right-skewed, since the mean of ARL_1 is much larger than the median for all situations. (ii) The CRPS chart is sensitive in detecting shifts in both the location and scale, but more sensitive in the latter. All simulated values decrease rapidly with only a small shift in θ and/or σ . Taking $m = 50$ as an example, ARL_1

decreases from 323.25 to 209.82 when θ increases from 0 to 0.1, while σ remains the same ($\sigma = 1$). However, it decreases from 323.25 to 72.98 when σ increases from 1 to 1.1, while θ remains 0. (iii) The CRPS chart has a better out-of-control performance as the sample size m increases. Similarly, taking $\theta = 0, 0.1$ and $\sigma = 1$, for example, we see that only a 10% rise on the location parameter θ brings a 35.1% reduction in ARL_1 when $m = 50$, as well as a 67% reduction for $m = 500$. This indicates that the CRPS chart becomes more sensitive at reducing ARL_1 , when it applies to large sample size.

In the second case, we repeat the above simulations with data from the Laplace distribution. Similarly, in-control samples are from Laplace(0, 1) and out-of-control samples are from a Laplace(θ, σ) distribution. For simplicity, we only take $m = 500$ and $ARL_0^* = 370$ as an example, and its corresponding LCL and UCL are found to be 0.1412 and 0.1979. Results are shown in Table A3. It indicates that all the characteristics decrease sharply as case (1) for the normal distribution. In addition, Figure 11 shows the falling speed of ARL_1 with an increasing shift

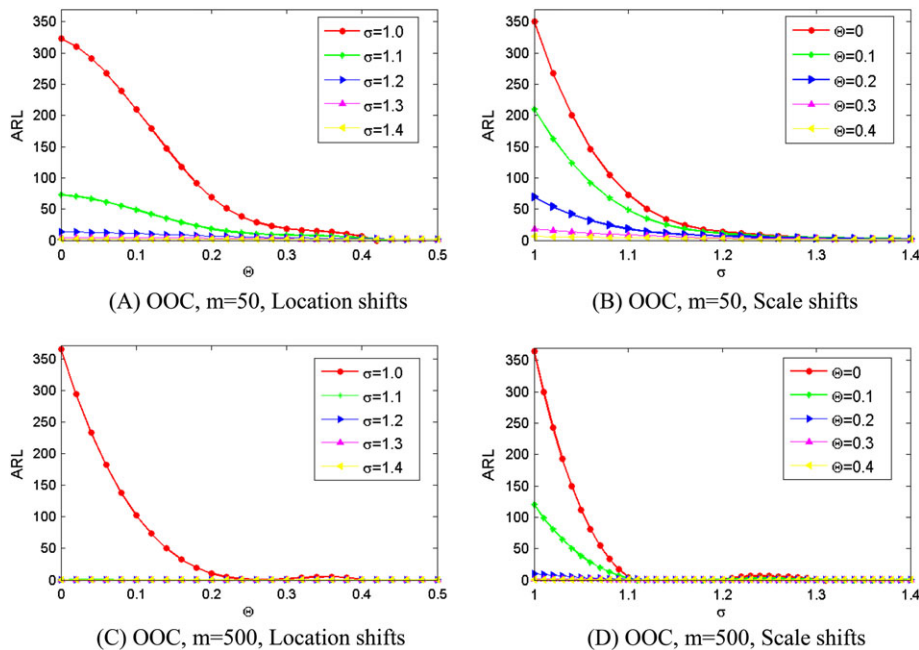


FIGURE 10 Out-of-control performances for the normal distribution [Colour figure can be viewed at wileyonlinelibrary.com]

in θ and σ . It is shown that the general pattern for the Laplace distribution remains the similar pattern as the case of the normal distribution.

6.3 | Performance comparison

It is useful to compare both performances of the CRPS chart with the existing (parametric and nonparametric) charts. First, we compare the CRPS chart with the parametric ELR chart (Zhang et al⁹). Then, the CRPS chart is compared with 2 competing nonparametric charts, the SL chart (Mukerjee and Chakraborti¹³) and the SC chart (Chowdhury et al¹⁵).

When comparing the CRPS chart with the ELR chart, in-control samples are generated from a standard normal distribution using simulations. Various magnitudes of shifts in the mean and variance are studied viz $\theta = 0, 0.25, 0.5, 0.75, 1.0, 2.0$ and $\sigma = 1, 1.2, 1.4, 1.6, 1.8, 2.0$. The ARL_0^* is taken as 370, and sample size is considered to be 5. Results of the mean and standard variation of ARL (SDRL) for both 2 charts are shown in Table A4. Table A4 shows that the ELR chart performs better than the CRPS chart for cases that shifts in both the mean and variance are less than one, since ARL of the ELR chart decreases faster than that of the CRPS chart. However, as shift increases, the 2 charts have comparable out-of-control performances and the CRPS charts begin to perform better than the ELR chart. For example, when the mean parameter shifts from 0 to 0.25, the ARL decreases sharply by 90.2% for ELR chart, and 71.1% for CRPS chart. Similarly, for a 20% increase in the variance, there is about 91.8% reduction in ARL for ELR chart, compared with a 72.4% reduction for the CRPS chart. This indicates that both the charts are more sensitive to shifts in the variance than in the mean. Finally, when both the mean and variance shift to 1, the ARL is 3.39 for the ELR chart, compared with 2.78 for the CRPS chart. As shift increases, the CRPS chart trends to perform better than the ELR chart in terms of both the mean and standard deviation of ARL.

We then compare the in-control performances of the CRPS chart with the SL and SC charts. For our

simulation study, all samples are from a standard normal distribution. The reference sample size m is set at 100 and 150, and sample size n is set at 5, 11, and 25. The target $ARL_0^* = 500$. Table 5 shows the results of the standard deviation (SDRL) and percentiles of ARL_0 for all the 3 charts. It is shown that the CRPS chart has the smallest SDRL value, indicating that the in-control performance of the CRPS chart is more stable compared with the SL and SC charts. Next, we study the out-of-control performances of the 3 charts. Both normal distribution and Laplace distribution are considered here. We only present $m = 100$ and $n = 5$. Control limits of the CRPS chart are obtained as 0.0828 and 0.7338 for the normal distribution, 0.0461 and 0.6785 for the Laplace distribution. Different shifts in location and scale are studied viz. $\theta = 0, 0.25, 0.5, 1.0$ and $\sigma = 1, 1.25, 1.5, 2.0$. Results are displayed in Tables A5 and A6, respectively, for the normal distribution and the Laplace distribution. Similar conclusions can be reached for the 2 different distributions, and we take the normal distribution as an example. As shift increases, all performance characteristics decrease sharply. However, those characteristics' decreasing speed varies for a same shift. For example, when there is a 25% increase in the location parameter (the scale parameter remains 1), ARL_1 mean dropped by 49.8% for the SL chart, 50.2% for the SC chart, and 56.3% for the CRPS chart. It indicates the CRPS chart has relatively better detection abilities than the SL and SC charts. In addition, a 25% increase in the scale parameter (the location parameter remains 0) brings a 79.9% reduction of ARL_1 for the SL chart, compared with 85.4% for the SC chart, and 79.3% for the CRPS chart. It shows that all the 3 charts detect a shift in the scale faster than that in the location. On the other hand, for all considered situations, the SDRL value of the CRPS chart is the smallest compared with the SL and SC charts. It indicates that the out-of-control performance of the CRPS chart is much more stable.

In summary, Tables A5 and A6 show that all of the SL, SC, and CRPS charts are reasonably effective for monitoring shifts in the location and scale, regardless the

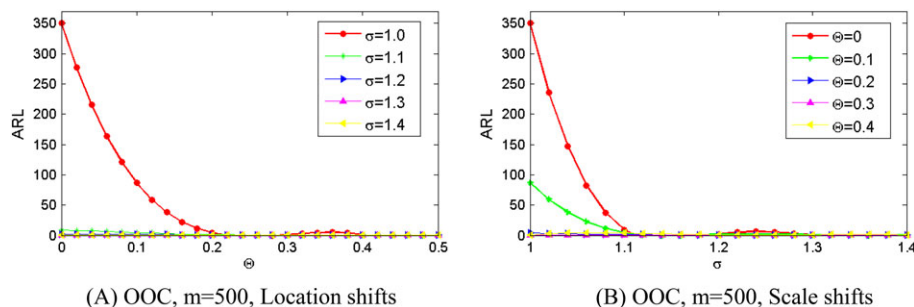


FIGURE 11 Out-of-control performances for the Laplace distribution [Colour figure can be viewed at wileyonlinelibrary.com]

TABLE 5 In-control performance comparisons among the SL, SC and CRPS charts with $ARL_0^* = 500$

Sample size		SL Chart	SC Chart	CRPS Chart
<i>m</i>	<i>n</i>			
100	5	690.00 (21,108,274,606,1710)	788.4 (15,95,253,604,1831)	461.88 (30,140,329,694,1433)
100	11	703.58 (18,99,281,611,1742)	886.1 (12,74,210,547,1900)	480.92 (29,157,279,633,1607)
100	25	703.81 (13,89,255,648,1837)	743.8 (12,78,243,621,1899)	450.68 (28,144,335,685,1390)
150	5	692.79 (18,113,287,632,1633)	723.9 (18,107,277,629,1737)	451.60 (31,142,305,700,1175)
150	11	627.38 (20,113,291,659,1675)	821.2 (15,87,237,575,1780)	473.26 (30,161,291,687,1595)
150	25	660.91 (16,95,272,645,1712)	688.5 (15,89,254,622,1780)	443.73 (31,156,349,718,1554)

The first number of each cell shows the SDRL, and parentheses () shows the 5th, 25th, 50th, 75th, and 95th of ARL_0 .

underlying distribution. The CRPS chart generally outperforms the SL and SC charts except for a small portion of the cases. When the shift is very small, the CRPS chart has no obvious advantages in the decreasing rate of ARL, but its stability is much better than the other 2 charts. As shift increases, the advantages of the CRPS chart are much more obvious in terms of both the decreasing rate of ARL and the stability. It is worth mentioning that when the sample size becomes larger, Section 6.2 illustrates that the CRPS chart also work well or even better.

7 | CONCLUSION

With the increasing complexity of industrial production system, large amounts of generated data have put forward higher challenges for process monitoring. Since the related literature on simultaneously monitoring the location and scale under data-rich environment is quite limited, this paper proposes a new control chart called the CRPS chart to fit in with the data-rich environment. The charting statistic is constructed based on the CRPS method, and control limits are determined by approximating the CRPS distribution via a gamma distribution. Both in-control and out-of-control performances are analyzed via the mean, the standard deviation, and some percentiles of the average run length distribution. In addition, both in-control and out-of-control performances of the CRPS chart are compared with the parametric ELR chart and the nonparametric SL and SC charts. Our results show that the proposed CRPS chart generally outperforms the competing distribution-free SL and SC charts.

The proposed CRPS chart has several clear advantages: (1) The CRPS chart can simultaneously monitor shifts in the location and/or the scale under data-rich environment. (2) There are no requirements based on the data distribution, both normal and nonnormal cases are equally applicable. (3) The CRPS chart is sensitive to both small and large shifts and can be used effectively

to detect shifts when the out-of-control process follows a different distribution from the in-control process.

ACKNOWLEDGEMENTS

The authors are grateful for the help and advice on this paper from Joe Gyekis (Pennsylvania State University). This research is supported by the National Natural Science Foundation of China (71532008).

REFERENCES

1. Wang K, Tsung F. Using profile monitoring techniques for a data-rich environment with large sample size. *Qual Reliabil Eng Int.* 2005;21:677-688.
2. Gan FF, Ting KW, Chang TC. Interval charting schemes for joint monitoring of process mean and variance. *Qual Reliabil Eng Int.* 2004;20:291-303.
3. McCracken AK, Chakraborti S. Control charts for joint monitoring of mean and variance: an overview. *Qual Technol Quantitative Mgmt.* 2013;10:17-35.
4. Chowdhury S, Mukherjee A, Chakraborti S. Distribution-free phase II CUSUM control chart for joint monitoring of location and scale. *Qual Reliabil Eng Int.* 2015;31:135-151.
5. Chen G, Cheng SW. Max Chart: combining X-bar and S chart. *Stat Sinica.* 1998;8:263-271.
6. Chen G, Cheng SW. Monitoring process mean and variability with one EWMA chart. *J Qual Technol.* 2001;33:223-233.
7. Costa AFB, Rahim MA. Monitoring process mean and variability with one non-central chi-square chart. *J Applied Stat.* 2004; 31:1171-1183.
8. Yeh AB, Lin DKJ, Venkataramani C. Unified CUSUM charts for monitoring process mean and variability. *Qual Technol Quantitative Mgmt.* 2004;1:65-86.
9. Zhang J, Zou C, Wang Z. A control chart based on likelihood ratio test for monitoring process mean and variability. *Qual Reliabil Eng Int.* 2010;26:63-73.
10. Cheng SW, Thaga K. Single variables control charts: an overview. *Qual Reliabil Eng Int.* 2006;22:811-820.

11. Zou C, Tsung F. Likelihood ratio-based distribution-free EWMA control charts. *J Qual Technol*. 2010;42:174-196.
12. Zhang J. Powerful goodness-of-fit tests based on likelihood ratio. *J Royal Stat Soc*. 2002;64:281-294.
13. Mukherjee A, Chakraborti S. A distribution-free control chart for the joint monitoring of location and scale. *Qual Reliabil Eng Int*. 2012;28:335-352.
14. Lepage Y. A combination of Wilcoxon's and Ansari-Bradley's statistics. *Biometrika*. 1971;58:213-217.
15. Chowdhury S, Mukherjee A, Chakraborti S. A new distribution-free control chart for joint monitoring of unknown location and scale parameters of continuous distributions. *Qual Reliabil Eng Int*. 2014;30:191-204.
16. Cucconi O. Un nuovo test non parametrico per il confront tra due gruppi campionari. *Giornale degli Economisti*. 1968; XXVII:225-248.
17. Brown TA. Admissible scoring systems for continuous distributions. *Math Models*. 1974;27.
18. Hersbach H. Decomposition of the continuous ranked probability score for ensemble prediction systems. *Weather and Forecasting*. 2000;15:559-570.
19. Thorarindottir TL, Gneiting T. Probabilistic forecasts of wind speed: ensemble model output statistics by using heteroscedastic censored regression. *J R Stat Soc A Stat Soc*. 2010;173:371-388.
20. Pinson P, Reikard G, Bidlot JR. Probabilistic forecasting of the wave energy flux. *Appl Energy*. 2012;93:364-370.
21. Shi L, Ma H, Lin DKJ. Process capability analysis via continuous ranked probability score. *Qual Reliabil Eng Int*. 2016;32: 2823-2834.
22. Friedman D. Effective scoring rules for probabilistic forecasts. *Mgmt Sci*. 1983;29:447-454.
23. Nau RF. Should scoring rules be effective? *Mgmt Science*. 1985;31:527-535.
24. Montgomery DC. *Introduction to Statistical Quality Control*. 4th ed. New York, NY: John Wiley; 2001.
25. Megahed FM, Wells LJ, Camelio JA, Woodall WH. A spatiotemporal method for the monitoring of image data. *Qual Reliabil Eng Int*. 2012;28:967-980.

Liangxing Shi is an Associate Professor in the Department of Industrial Engineering at Tianjin University, China. He received his PhD from Tianjin University in 2008. His research interests include quality engineering, six sigma, industrial engineering, and operations management.

Ling Gong is a Master candidate in the Department of Industrial Engineering at Tianjin University, China. Her research interests focus on quality management and industrial engineering.

Dennis K. J. Lin is a Distinguished Professor of Statistics and Supply Chain Management at the Pennsylvania State University, USA. He received his PhD in Statistics from the University of Wisconsin, Madison, USA, in 1988. His research interests are quality assurance, industrial statistics (design of experiment, reliability, statistical process control, quality assurance), data mining, and response surface.

How to cite this article: Shi L, Gong L, Lin DKJ. CRPS chart: Simultaneously monitoring location and scale under data-rich environment. *Qual Reliabil Engng Int*. 2018;34:681-697. <https://doi.org/10.1002/qre.2280>

APPENDIX A

TABLE A1 Out-of-control performance characteristics of ARL_1 for the normal distribution with $ARL_0^* = 370$ and $m = 50$

θ	σ	Mean	SD	5 th	25 th	Median	75 th	95 th
0	1	323.25	331.8	15.5	92	219	440	1051
0.1	1	209.82	211.63	10.5	58	150	287.5	642
0.2	1	68.59	70.15	4	19.5	47.5	93.5	208
0.3	1	18.80	18.73	1	5	13	26	56
0.4	1	6.37	5.93	1	2	4	9	18
0	1.1	72.98	77.33	4.5	21	50	98	216.5
0.1	1.1	48.58	44.44	3	16	36	69	138.5
0.2	1.1	18.28	18.07	2	5	12	25	55

TABLE A1 (Continued)

θ	σ	Mean	SD	5 th	25 th	Median	75 th	95 th
0.3	1.1	8.41	8.16	1	3	6	11	24
0.4	1.1	3.96	3.44	1	1	3	5	11
0	1.2	13.64	13.53	1	4	9.5	19	43
0.1	1.2	10.99	10.88	1	3	8	15	33
0.2	1.2	6.84	6.34	1	2	5	10	18
0.3	1.2	3.97	3.41	1	1	3	5	11
0.4	1.2	2.53	1.87	1	1	2	3	6
0	1.3	4.51	3.81	1	2	3	6	12
0.1	1.3	4.24	3.89	1	1.5	3	5	12
0.2	1.3	3.37	2.82	1	1	3	4	9
0.3	1.3	2.39	1.78	1	1	2	3	6
0.4	1.3	1.78	1.13	1	1	1	2	4
0	1.4	2.34	1.80	1	1	2	3	6
0.1	1.4	2.21	1.62	1	1	2	3	6
0.2	1.4	1.99	1.36	1	1	2	3	5
0.3	1.4	1.63	1.02	1	1	1	2	4
0.4	1.4	1.38	0.72	1	1	1	2	3

TABLE A2 Out-of-control performance characteristics of ARL_1 for the normal distribution with $ARL_0^* = 370$ and $m = 500$

θ	σ	Mean	SD	5 th	25 th	Median	75 th	95 th
0	1	364.75	366.85	20.5	96	249	497.5	1166.5
0.1	1	120.28	120.72	8	35.5	84	164.5	382.5
0.2	1	10.42	10.35	1	3	7	14	30
0.3	1	1.84	1.25	1	1	1	2	4
0.4	1	1.05	0.21	1	1	1	1	1
0	1.1	4.32	3.89	1	2	3	6	13
0.1	1.1	2.84	2.28	1	1	2	4	7
0.2	1.1	1.51	0.84	1	1	1	2	3
0.3	1.1	1.07	0.26	1	1	1	1	2
0.4	1.1	1.00	0.32	1	1	1	1	1
0	1.2	1.10	0.33	1	1	1	1	2
0.1	1.2	1.09	0.32	1	1	1	1	2
0.2	1.2	1.02	0.141	1	1	1	1	1
0.3	1.2	1	0	1	1	1	1	1
0.4	1.2	1	0	1	1	1	1	1
0	1.3	1	0.04	1	1	1	1	1
0.1	1.3	1	0.03	1	1	1	1	1
0.2	1.3	1	0	1	1	1	1	1
0.3	1.3	1	0	1	1	1	1	1
0.4	1.3	1	0	1	1	1	1	1

TABLE A2 (Continued)

θ	σ	Mean	SD	5th	25th	Median	75th	95th
0	1.4	1	0	1	1	1	1	1
0.1	1.4	1	0	1	1	1	1	1
0.2	1.4	1	0	1	1	1	1	1
0.3	1.4	1	0	1	1	1	1	1
0.4	1.4	1	0	1	1	1	1	1

TABLE A3 Out-of-control performance characteristics of ARL_1 for the Laplace distribution with $ARL_0^* = 370$ and $m = 500$

θ	σ	Mean	SD	5th	25th	Median	75th	95th
0	1	350.14	336.96	19	111	256	474.5	1059.5
0.1	1	86.59	85.13	5	24	59	125	256.5
0.2	1	4.222	3.56	1	2	3	6	12
0.3	1	1.16	0.44	1	1	1	1	2
0.4	1	1.0	0.04	1	1	1	1	1
0	1.1	9.1	8.49	1	3	7	12	26
0.1	1.1	4.41	3.75	1	2	3	6	12
0.2	1.1	1.46	0.77	1	1	1	2	3
0.3	1.1	1.02	0.14	1	1	1	1	1
0.4	1.1	1	0	1	1	1	1	1
0	1.2	1.60	0.93	1	1	1	2	4
0.1	1.2	1.34	0.70	1	1	1	1	3
0.2	1.2	1.07	0.26	1	1	1	1	2
0.3	1.2	1	0.03	1	1	1	1	1
0.4	1.2	1	0	1	1	1	1	1
0	1.3	1.05	0.23	1	1	1	1	1
0.1	1.3	1.03	0.16	1	1	1	1	1
0.2	1.3	1	0.03	1	1	1	1	1
0.3	1.3	1	0	1	1	1	1	1
0.4	1.3	1	0	1	1	1	1	1
0	1.4	1	0.07	1	1	1	1	1
0.1	1.4	1	0	1	1	1	1	1
0.2	1.4	1	0	1	1	1	1	1
0.3	1.4	1	0	1	1	1	1	1
0.4	1.4	1	0	1	1	1	1	1

TABLE A4 Out-of-control performance comparisons between the ELR chart and CRPS chart for a normal distribution with $ARL_0^* = 370$

Shifts	Mean	Variance	ELR chart		CRPS chart	
			ARL	SDRL	ARL	SDRL
0	0	1	370	369	373.4	371.2
		1.2	30.3	26.9	103.2	114.4
		1.4	8.58	6.17	27.4	30.4
		1.6	4.62	2.9	12.1	12.2
		1.8	3.2	1.87	5.18	4.72
		2.0	2.46	1.36	3.82	3.78
0.25	0.25	1	36.5	31.6	107.84	110.36
		1.2	16.2	12.9	45.29	46.68
		1.4	7.18	4.88	20.22	22.16
		1.6	4.28	2.61	10.12	10.87
		1.8	3.06	1.78	4.74	3.75
		2.0	2.40	1.31	3.12	2.53
0.5	0.5	1	9.41	5.61	20.84	17.56
		1.2	7.46	4.77	13.84	11.71
		1.4	5.12	3.12	6.28	5.63
		1.6	3.66	2.13	5.34	4.23
		1.8	2.78	1.56	3.96	3.29
		2.0	2.26	1.23	2.52	2.03
0.75	0.75	1	5.01	2.27	6.66	6.02
		1.2	4.51	2.34	5.56	5.47
		1.4	3.69	2	3.82	3.12
		1.6	2.97	1.62	3.66	2.90
		1.8	2.46	1.32	3.38	2.57
		2.0	2.08	1.10	1.94	1.28
1	1	1	3.39	1.35	2.78	1.91
		1.2	3.18	1.47	2.34	1.63
		1.4	2.84	1.39	2.28	1.61
		1.6	2.46	1.26	2.02	1.61
		1.8	2.13	1.09	2.10	1.43
		2.0	1.90	0.97	1.68	1.12
2	2	1	1.50	0.54	1.09	0.32
		1.2	1.46	0.56	1.07	0.26
		1.4	1.42	0.56	1.06	0.24
		1.6	1.39	0.56	1.05	0.22
		1.8	1.35	0.54	1.03	0.17
		2.0	1.31	0.52	1.01	0.1

Scenarios where the CRPS chart is superior are highlighted in bold.

TABLE A5 Out-of-control performance comparisons among the SL, SC, and CRPS charts for the normal distribution with $ARL_0^* = 500$

Shifts				
Location	Scale	SL Chart	SC Chart	CRPS Chart
0	1	513.0(738.9)18,106,276,635,1792	509.4(788.4)15,95,253,604,1831	490.73(461.88)30,140,329,694,1433
0.25	1	257.6(410.3)9,47,127,303,917	253.6(456.4)8,43,116,285,935	212.47(188.95)14,66,149,298,581
0.5	1	66.5(98.6)3,13,35,80,237	68.6(117.2)3,14,34,80,239	34.97(35.26)1.5,10,26,50,104
1	1	7.7(8.8)1,2,5,10,24	7.7(9.4)1,2,5,10,24	2.7(3.1)1,1,1,4,10
0	1.25	102.9(124.1)5,25,62,133,337	74.5(92.2)3,18,45,96,243	100.6(107.2)2,24,71,128,370
0.25	1.25	70.6(92.3)3,17,41,89,232	54.9(70.8)3,13,32,69,183	51.1(49.3)2,15,34,74,151
0.5	1.25	30.9(38.8)2,8,18,40,101	26.2(32.4)1,7,15,34,86	15.1(20.2)1,5,10,19,38
1	1.25	6.7(7.0)1,2,4,9,20	6.2(6.6)1,2,4,8,19	2.1(2.5)1,1,1,3,8
0	1.5	37.5(42.2)2,10,24,50,118	24.3(27.1)2,6,16,32,76	26.1(30.3)1,6,18,33,102
0.25	1.5	29.9(34.2)2,8,19,39,91	20.4(22.7)1,6,13,27,64	18.9(19.8)1,4,12,29,63
0.5	1.5	17.8(19.7)1,5,12,24,55	13.4(15.1)1,4,9,17,42	8.6(8.9)1,2,6,12,24
1	1.5	6.1(6.1)1,2,4,8,18	5.3(5.3)1,2,4,7,15	2.0(2.0)1,1,1,3,6
0	2	11.5(11.9)1,3,8,15,35	7.1(6.9)1,2,5,10,21	3.7(3.8)1,1,3,6,11
0.25	2	10.8(10.9)1,3,7,15,32	6.8(6.6)1,2,5,9,20	3.2(3.5)1,0.5,2,5,9.5
0.5	2	8.6(8.5)1,3,6,11,25	5.8(5.7)1,2,4,8,17	2.7(3.0)1,1,1.5,4,9
1	2	4.8(4.5)1,2,3,6,14	3.8(3.4)1,1,3,5,11	1.4(1.8)1,1,1,2,5

The first number of each cell shows the mean of ARL_1 , parentheses () indicates the SDRL value, and the last five numbers of each cell show the 5th, 25th, 50th, 75th, and 95th of ARL_1 ; scenarios where the CRPS chart is superior are highlighted in bold.

TABLE A6 Out-of-control performance comparisons between the SL, SC, and CRPS charts for the Laplace distribution with $ARL_0^* = 500$

Shifts				
Location	Scale	SL Chart	SC Chart	CRPS Chart
0	1	508.3.2(728.1)18,106,277,626,1742	509.6(817.7)15,93,251,589,1909	486.29(456.67)27,153,349,686,1645
0.25	1	366.9(589.4)11,64,177,440,1318	381.6(758.8)11,63,175,429,1351	225.4(198.67)7.5,71,167,337,629
0.5	1	159.2(286.2)5,25,68,174,608	191.0(482.9)5,25,73,191,722	30.4(38.9)2.5,9,17,35.5,99
1	1	19.9(37.3)1,4,9,21,73	26.5(86.1)1,4,11,27,95	2.4(1.82)1,1,2,3,7
0	1.25	153.2(198.4)6,35,88,197,512	124.5(173.2)5,27,68,150,437	90.2(88.94)7,22,60,131,291
0.25	1.25	121.5(161.6)5,26,68,153,422	100.6(145.6)4,21,54,122,345	41.78(46.3)4,11,27,52,134
0.5	1.25	66.19(103.7)3,13,35,78,227	61.7(101.9)3,12,31,73,215	17.6(17.5)1,5,12,24,51
1	1.25	14.0(19.6)1,3,8,17,47	14.6(22.2)1,3,8,17,50	2.1(1.6)1,1,1.5,2.5,5.5
0	1.5	66.8(80.5)4,17,41,86,218	47.8(59.7)2,12,29,61,156	26.8(21.8)4,12,20,37,79
0.25	1.5	55.2(65.6)3,14,33,72,184	42.1(52.4)2,10,25,53,139	22.3(24.4)2,7,16,30,66
0.5	1.5	36.8(46.7)2,8,22,46,124	29.6(39.1)2,7,17,37,101	9.4(7.9)1,3,7,14,24
1	1.5	11.1(14.2)1,3,7,14,36	10.7(15.2)1,3,6,13,34	2.3(1.9)1,1,2,3,6
0	2	22.9(25.3)2,6,15,31,71	14.5(16.2)1,4,9,19,45	5.7(5.1)1,2,5,7,17
0.25	2	21.1(23.5)1,6,14,28,66	13.6(15.1)1,4,9,18,43	5.2(4.6)1,2,4,7,14
0.5	2	16.6(18.1)1,5,11,22,51	11.3(12.4)1,3,7,15,35	4.6(4.1)1,2,3,7,15
1	2	7.9(8.7)1,2,5,10,25	6.3(6.7)1,2,4,8,19	1.9(1.2)1,1,1,2,4.5

The first number of each cell shows the mean of ARL_1 , parentheses () indicates the SDRL value, and the last five numbers of each cell show the 5th, 25th, 50th, 75th, and 95th of ARL_1 ; scenarios where the CRPS chart is superior are highlighted in bold.